Compensatory changes in GroEL/Gp31 affinity as a mechanism for allele-specific genetic interaction

Richardson, A.; van der Vies, S.; Keppel, F.; Taher, A.; Landry, S.J.; Georgopoulos, C.

published in
Journal of Biological Chemistry
1999

DOI (link to publisher)
10.1074/jbc.274.1.52

document version
Publisher's PDF, also known as Version of record

THE JOURNAL OF BIOLOGICAL CHEMISTRY
Vol. 274, No. 1, Issue of January 1, pp. 52–58, 1999

Printed in U.S.A.

Compensatory Changes in GroEL/Gp31 Affinity as a Mechanism for Allele-specific Genetic Interaction*

(Received for publication, August 24, 1998, and in revised form, October 5, 1998)

Alexandra Richardson‡§, Saskia M. van der Vies‡¶, France Keppel‡, Abida Taher‖, Samuel J. Landry‖, and Costa Georgopoulos‡

From the ‡Département de Biochimie Médicale, University of Geneva, 1 rue Michel-Servet, 1211 Geneva, Switzerland and ‖Department of Biochemistry, Tulane University School of Medicine, New Orleans, Louisiana 70112

Previous work has shown that the GroEL-GroES interaction is primarily mediated by the GroES mobile loop. In bacteriophage T4 infection, GroES is substituted by the gene *31*-encoded cochaperonin, Gp31. Using a genetic selection scheme, we have identified a new set of mutations in gene *31* that affect interaction with GroEL; all mutations result in changes in the mobile loop of Gp31. Biochemical analyses reveal that the mobile loop mutations alter the affinity between Gp31 and GroEL, most likely by modulating the stability of the GroEL-bound hairpin conformation of the mobile loop. Surprisingly, mutations in *groEL* that display allele-specific interactions with mutations in gene *31* alter residues in the GroEL intermediate domain, distantly located from the mobile loop binding site. The observed patterns of genetic and biochemical interaction between GroES or Gp31 and GroEL point to a mechanism of genetic allele specificity based on compensatory changes in affinity of the protein-protein interaction. Mutations studied in this work indirectly alter affinity by modulating a folding transition in the Gp31 mobile loop or by modulating a hinged conformational change in GroEL.

Chaperonin-assisted folding of certain substrates depends on the coordinated interaction of GroEL, ATP, and GroES (1, 2). Certain unfolded or partially folded polypeptides bind to GroEL, a double-toroid, tetradecameric protein composed of 58-kDa subunits arranged with 7-fold symmetry (3–5). GroES, made up of 10.5-kDa subunits arranged in 7-fold symmetry (6, 7), binds to GroEL, thus stabilizing a conformational change that doubles the substrate-containing cavity of GroEL and promoting the release of the substrate into the cavity (8, 9). The amount of time the substrate spends in the cavity depends on the rate of ATP hydrolysis in the GroEL *cis* ring and the release of GroES (10, 11). In turn, the release of GroES is promoted by the binding of ATP or ATP and GroES to the *trans* GroEL ring (11, 12). After GroES release, the polypeptide substrate is released either in a folded or a folding-competent state or in a conformation still recognizable by GroEL, in which case it binds to the same or a different GroEL molecule (13). The efficient cycling of the GroE chaperone machine is essential to ensure that the chaperonin can provide the necessary folding assistance to its substrates (14–16).

GroEL is essential for bacteriophage T4 growth. The mutant *groEL44*(E191G) allele has been shown to block bacteriophage T4 growth at the level of capsid head assembly, *i.e.* in *groEL44*(E191G) mutant cells, Gp23, the major capsid protein, aggregates into amorphous lumps (17). The same phenotype was previously observed during infection of a wild type host by a bacteriophage T4 defective in gene *31* (18). Subsequent analyses of genetic suppressors identified an interaction between the host *groEL* gene and the bacteriophage T4 gene *31* (19).

It turned out that Gp31 is functionally analogous to GroES despite low sequence identity (14% at the amino acid level) (20, 21), and it can completely replace GroES for *Escherichia coli* growth.[1] The crystal structures of GroES and Gp31 reveal significant structural identities as expected from their similar *in vivo* and *in vitro* function (6, 22). Both GroES and Gp31 subunits bear a flexible polypeptide segment, identified by nuclear magnetic resonance (NMR) spectroscopy and limited proteolysis (23, 24). The mobile loops mediate GroEL-GroES binding through a central hydrophobic tripeptide (Ile^{25}-Val^{26}-Leu^{27}) as shown by NMR studies and confirmed by the crystal structure of the GroEL·ADP·GroES complex (8, 23).

All mutations identified thus far in either *groES* or gene *31*, which result in defective GroEL interaction, alter amino acid residues in the mobile loop. Interestingly, most of these GroES substitutions do not affect the IVL tripeptide. Rather, the best characterized *groES* mutant alleles affect either of the two glycine residues preceding the IVL residues (25) and that participate in formation of a β-hairpin turn (24). Bacteriophage T4 gene *31* mutant alleles affect a number of residues in the mobile loop including residue Leu^{35}, corresponding to Ile^{25} in the GroES mobile loop (26).

Mutations in *groEL*, originally identified on the basis of blocking bacteriophage growth, affect residues that are distant from the mobile-loop binding site. The affected residues lie in the intermediate domain that links the ATP binding equatorial domain with the substrate and GroES binding apical domain (23). The GroEL·ADP·GroES crystal structure revealed that the intermediate segment, in fact, provides two hinges that allow for the large *en bloc* movements in GroEL, which are captured by GroES binding (8). Genetic analyses have revealed that *groEL* mutations fall into two classes on the basis of their allele-specific interaction with *groES* (25, 27) or gene *31* (17) mutations. The study concerning GroEL-Gp31 interaction revealed that of two *groEL* mutants that block bacteriophage λ growth, *groEL44*(E191G) and *groEL515*(A383T), only the former blocks bacteriophage T4 growth. Surprisingly, mutations in gene

* This work was supported by the Canton of Geneva, Swiss National Foundation Grant 31.47283-96 and National Science Foundation Grant MCB-9512711. The costs of publication of this article were defrayed in part by the payment of page charges. This article must therefore be hereby marked "*advertisement*" in accordance with 18 U.S.C. Section 1734 solely to indicate this fact.

§ To whom correspondence should be addressed. Tel.: 41-22 702 55 07; Fax: 41-22 702 55 02; E-mail: Alexandra.Richardson@medecine.unige.ch.

¶ Present address: Faculty of Chemistry, Free University Amsterdam, De Boelelaan 1083, 1081 HV Amsterdam, The Netherlands.

[1] F. Keppel, unpublished data.

31, that restore bacteriophage T4 growth on *groEL44*(E191G), simultaneously prevent plaque formation on *groEL515*(A383T).

Understanding how specific mutations in these genes affect chaperone function is the overall aim of the work described in this paper. Taking advantage of a simple genetic selection system, we have identified new mutations in gene *31* of bacteriophage T4 that switch the phenotype from suppression of *groEL44*(E191G) to suppression of *groEL515*(A383T). Biochemical analyses reveal that these gene *31* mutations exert their effects primarily by altering the affinity of Gp31 for GroEL.

EXPERIMENTAL PROCEDURES

Genetic Selection—Twenty independent lysates of the original T4ϵ1(Gp31(L35I)) mutant were plated separately on *groEL515*(A383T) bacteria. Plaque formers, occurring at a frequency of approximately 10^{-6} were isolated, restreaked, and characterized for plating ability on different *groEL* mutant hosts. The minimal gene *31* was amplified by polymerase chain reaction using Dynazyme *Taq* polymerase from a plaque isolated from a *groEL515*(A383T) lawn, and the polymerase chain reaction product was sequenced directly using the Amersham Pharmacia Biotech Delta *Taq* sequencing kit (28). All 20 suppressors sequenced contained the original ϵ1 mutation (L35I) and in addition had a mutation that altered a second amino acid residue, also localized in the mobile loop. Twelve of these pseudorevertants had a mutation that resulted in a change at codon 31 of Thr to Ala, and two candidates had a change at the same site from a Thr to an Ile.

Cloning of Wild Type and Mutant Genes—Mutant gene *31*(L35I, T31A) was amplified by polymerase chain reaction; the polymerase chain reaction fragment was cloned into the *Eco*RI and *Xba*I sites of the high copy pBAD vector pMPM201 (29), and the resulting clone overproducing Gp31(L35I,T31A) was named pALEX5. The wild type gene *31* was cloned in the same manner, except the amplification was done from a wild type T4 plaque isolated on a B178 lawn, and the resulting clone was named pALEX1. The Gp31(I36W) protein was overproduced from pALEX32, created by the introduction of the corresponding mutation, resulting in I36W by site-directed mutagenesis (30) using pALEX1 as the template. Mutant gene *31* (L35I) was made by site-directed mutagenesis (30) using the plasmid pSV25 (wild type gene *31*) as the template (20). All clones were sequenced in their entirety using either the standard Sanger sequencing method or automated sequencing (Li-CORE).

pBAD*groESgroEL* is a plasmid that expresses the wild type *groES* and *groEL* genes under the control of the arabinose-induced promoter. The *groES* and *groEL* genes were cloned as a 2.1-kilobase pair fragment from pOFx62(27) containing 45 base pairs upstream of the starting ATG codon. The fragment was cloned into pBAD22 (31).

Plasmid pBAD*groESgroEL*(A383T), used to overexpress GroEL-(A383T), was constructed by replacing the *Bst*XI-*Sma*I fragment from pBAD*groESgroEL* with the corresponding *Bst*XI-*Sma*I fragment from plasmid pOF1153 (27). The authenticity of the clone was verified by sequencing 300 base pairs around the altered codon.

Protein Purification—Wild type GroEL and GroES were overexpressed from pBAD*groESgroEL* transformed into MC1009 cells and induced with arabinose and purified essentially as described previously (23). Residual peptides bound to GroEL were removed by Affi-Gel Blue chromatography in the presence of buffer containing 50 mM Tris-HCl, pH 7.5, 125 mM NaCl, 1 mM ATP, and 2.5 mM $MgCl_2$ followed by MonoQ chromatography to remove GroEL-associated nucleotide (buffer: 20 mM Bis-Tris, pH 6.0, 50 mM-1M KCl gradient).

GroEL(A383T) was overproduced from pBAD*groESgroEL*(A383T) transformed into *groEL515*(A383T) cells, and GroEL(E191G) was overproduced from pJZ548(27) transformed into the *groEL44*(E191G) mutant background. Both mutant proteins were purified following the same procedure as that used for wild type GroEL.

Gp31, Gp31(L35I), Gp31(L35I,T31A), and Gp31(I36W) were purified from the overexpressing plasmids described above, all in the MC1009 genetic background. The purification procedures used were identical to those previously described (20). The expected molecular mass of wild type Gp31, Gp31(L35I,T31A), and Gp31(I36W) were confirmed by electrospray mass spectroscopy.

All proteins were stored at −80 °C in a buffer containing 50 mM Tris-HCl, pH 7.5, 1 mM EDTA, 1 mM dithiothreitol, and 15% (v/v) glycerol. Protein concentrations were measured by either absorption at 280 nm using molar extinction coefficients determined by quantitative amino acid analysis or by the Bradford protein assay method, standardized with known concentrations of either GroEL or Gp31.

Citrate Synthase Refolding—The chaperonin-dependent renaturation of pig heart citrate synthase (referred to in the text as citrate synthase) was performed as described previously (32). The following protein concentrations (given for monomers) were used: 4.2 μM chaperonins and cochaperonins and 0.2 μM citrate synthase. Citrate synthase at 33 μM was denatured for 30–60 min at 27 °C in a solution containing 6 M guanidine hydrochloride, 3 mM dithiothreitol, and 2 mM EDTA. The refolding buffer contained 10 mM $MgCl_2$, 2 mM ATP, 1 mM oxaloacetic acid, and 20 mM potassium phosphate, pH 7.4. The refolding reaction was performed at 27 °C in a total volume of either 200 μl or 400 μl, and citrate synthase activity was measured after 60 min.

Complex Formation—Complex formation was initiated by adding ATP to a final concentration of 1 mM to a solution containing 50 mM Tris-HCl, pH 7.7, 7.8 mM $MgCl_2$, 1 mM KCl, 1 mM dithiothreitol, 8.4 μM GroEL, and 35.2 μM Gp31 (monomers). The reaction mixture (250 μl) was left at 22 °C for 10 min. An aliquot of 200 μl was loaded onto a TSK 3000G gel-fitration column that had been equilibrated in 50 mM Tris-HCl, pH 7.7, 10 mM $MgCl_2$, 1 mM KCl, 0.01% (w/v) Tween 20, and 0.23 mM ATP. The column was run at 22 °C at a flow rate of 1 ml/min. The fraction between 10.5 and 11.5 min was collected. Samples were acetone-precipitated and analyzed by means of electrophoresis on a 15% polyacrylamide gel containing SDS. The proteins were stained with Coomassie Brilliant Blue.

Fluorescence Experiments—A Photon Technologies Inc. Quanta Master luminescence spectrometer with a double excitation set-up and gloved cuvette holder maintained at 25 °C with a cooler-heater water bath system was used for fluorescence analysis. All reactions were performed under constant stirring and in a total volume of 2 ml. The intensity at 337 nm was monitered as a function of time with excitation at 295 nm and all slits adjusted to 4 nm. The following protein concentrations were used (in monomers): 2.0 μM GroEL, 1.4 μM Gp31(I36W), and 1.4 μM Gp31 and its mutant variants. ATP was used at 1 mM with a buffer containing 100 mM Tris-HCl, pH 7.5, 1 mM $MgCl_2$, and 1 mM dithiothreitol. Data were initially analyzed in Felix software provided with the spectrometer and converted into a Kaleidagraph for presentation. The background fluorescence intensity contribution associated with nontryptophan-containing proteins (expressed as a percentage of the fluorescence intensity for Gp31(I36W) alone)) was subtracted accordingly: GroEL, 20%; Gp31, 8%, Gp31(L35I), 5%; Gp31(L35I,T31A), 6%.

Transferred Nuclear Overhauser Effect (trNOE)[2] NMR Analysis—Carboxamide peptides corresponding to the mobile loops of Gp31, Gp31(L35I), and Gp31(L35I,T31A) were synthesized using 9-fluorenylmethoxycarbonyl chemistry, acetylated off-line, and purified by reverse-phase high preformance liquid chromatography. Sequences are as follows: Gp31, AQAGDEEVTESGLIIGKRVQ; GP31(L35I), AQAGDEEVTESGIIIGKRVQ; GP31(L35I,T31A), AQAGDEEVAESGIIIGKRVQ. Peptide sequences were confirmed by matrix-assisted laser desorption ionization mass spectrometry (MALDI). GroEL and GroEL(E191G) were exchanged and concentrated into a 50 mM potassium phosphate, pH 6.1, buffer (Centricon-30, Amicon). GroEL was added to a final concentration of 60 μM in an NMR sample containing 2 mM peptide, 10% D_2O, and 0.3 mM trimethylsilyl proprionate in 50 mM potassium phosphate, pH 6.1, buffer. Spectra were recorded at 30 °C on a General Electric OMEGA PSG 500 NMR spectrometer operating at 500.05 MHz frequency. Data were processed as described previously (24) using Felix software (Biosym Technologies, San Diego, CA) running on a Silicon Graphics Indigo (Mountain View, CA) work station.

RESULTS

groEL/Gene 31 Allele-specific Mutations Fall into Two Classes—Previous work has shown that bacteriophage T4 mutations, which restore growth on *groEL44*(E191G) map to gene *31* (17), and sequencing of one candidate, called T4ϵ1, showed that the mutation in gene *31* results in an amino acid change at codon 35 from Leu to Ile (26). This apparently subtle change in Gp31 resulted in a strikingly different genetic interaction with GroEL, because T4ϵ1 simultaneously lost its ability to plaque on *groEL515*(A383T) mutant bacteria. We took advantage of the finding that T4ϵ1 does not grow on *groEL515*(A383T) mutant bacteria to isolate spontaneously occurring, bacterio-

[2] The abbreviation used is: trNOE, transferred nuclear Overhauser effect.

TABLE I
Plating ability of various bacteriophage T4 mutant strains at 37 °C

The ability of bacteriophage T4 wild type and its gene *31* mutant derivatives to form plaques on various *E. coli* hosts at an approximate efficiency of 1.0 is denoted as +. The inability to form plaques on a given bacterial host is denoted as −. However, at a frequency of 10^{-6}–10^{-7}, spontaneously occurring revertants can be isolated as plaque-formers on the various nonpermissive bacterial hosts.

	groEL wild type	*groEL44* (E191G)	*groEL515* (A383T)
T4 wild type	+	−	+
T4 *31*(L35I)	+	+	−
T4 *31*(L35I,T31A) 12 of 20 isolates	+	−	+
T4 *31*(L35I,T31I) 2 of 20 isolates	+	−	+

phage-encoded suppressors. From 20 independent T4ϵ1 lysates plated on *groEL515*(A383T), bacteriophage "revertants" capable of forming a plaque were isolated at a frequency of approximately 10^{-6}. All revertants simultaneously lost their capacity to propagate on *groEL44*(E191G) mutant bacteria. Sequence analysis showed that all 20 candidates retain the original ϵ1 mutation (Leu to Ile at codon 35). The most frequently occurring suppressor mutation (12 of 20 isolates) resulted in a substitution at codon 31 of Thr with Ala, and two additional revertants were shown to alter the same codon to an Ile (Table I). Significantly, the genetic interaction between residues 35 and 31 in the mobile loop of Gp31 coincides with the physical interaction observed in the GroEL-bound conformation determined by trNOE NMR (Fig. 5*B*) (24).

Mutations in groEL and Gene 31 Affect Chaperonin-assisted Refolding of Citrate Synthase—Previous work has shown that citrate synthase depends on both GroEL and GroES for renaturation (32). In the absence of chaperonins, only 10–20% of denatured citrate synthase regains activity. GroEL alone (with ATP) inhibits refolding of citrate synthase (Fig. 1). In contrast, GroEL paired with GroES, Gp31, Gp31(L35I), or Gp31(L35I, T31A) efficiently helps citrate synthase refolding. Likewise, GroEL(E191G) inhibits refolding of the substrate in the absence of a cochaperonin but assists citrate synthase refolding with GroES. However, when paired with Gp31, GroEL(E191G) is unable to assist refolding. As anticipated from our *in vivo* genetic analysis, Gp31(L35I) restores chaperonin-assisted folding by GroEL(E191G), whereas Gp31(L35I,T31A) and GroEL(E191G) form a nonfunctional pair for the refolding of citrate synthase.

The above results indicate that citrate synthase refolding depends on functional interaction between GroEL and Gp31, strongly suggesting that the observed defects in bacteriophage T4 growth are also the result of aberrant chaperone-assisted folding. What is the molecular basis of the defect in chaperonin-cochaperonin interaction? The amino acid substitutions in Gp31 or GroEL could increase or decrease their affinity for each other. To test this, we analyzed complex formation by gel filtration chromatography.

The L35I Substitution in Gp31 Restores Binding to GroEL(E191G)—Formation of the GroEL·Gp31 complex requires nucleotide and can be observed by size fractionation on gel filtration chromatography (Fig. 2*A*). With the same conditions, GroEL(E191G) does not form a complex with Gp31 (Fig. 2*B*). Therefore, the inability of GroEL(E191G) to assist citrate synthase refolding when paired with Gp31 is most likely because of a lack of stable chaperonin-cochaperonin complex formation. However, GroEL(E191G)·ATP does form a stable complex with Gp31(L35I) (Fig. 2*C*). Thus, we conclude that the substitution in Gp31(L35I) increases the affinity of Gp31 affinity for GroEL, and we hypothesize that Gp31(L35I,T31A) decreases the affinity of Gp31 for GroEL. To test this, we developed a technique to distinguish subtle differences in GroEL binding between Gp31 and Gp31 mutants.

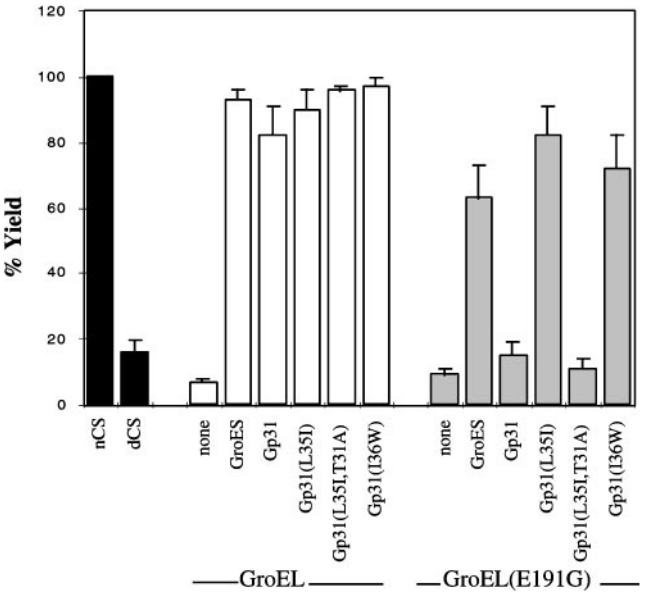

FIG. 1. **Chaperonin-dependent refolding of citrate synthase.** The yield of folded protein is expressed as a percentage of nondenatured citrate synthase activity. Citrate synthase activity was measured after 60 min of refolding at 27 °C with the indicated combinations of chaperones, as described under "Experimental Procedures." Data presented are the average and S.E. of three separate experiments.

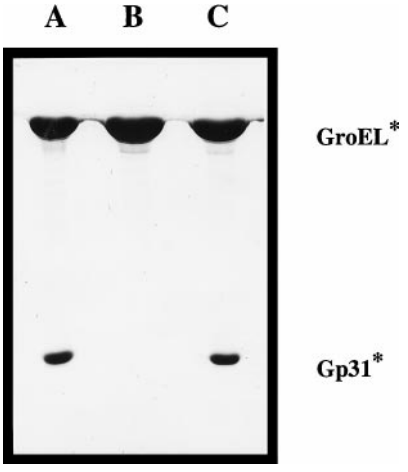

FIG. 2. **Complex formation of mutant and wild type GroEL and Gp31 proteins.** A Commassie Brilliant Blue-stained gel is presented showing the proteins present in the GroEL-containing fraction following chromatography on a TSK 3000G column. *Lanes* represent mixtures containing: *A*, GroEL and Gp31; *B*, GroEL(E191G) and Gp31; *C*, GroEL(E191G) and Gp31(L35I). The *asterisk* (*) indicates either wild type or mutant protein.

Relative GroEL-binding Affinities of Gp31 Mutants Determined by Competition with a Fluorescent Gp31 Variant—Tryptophan fluorescence may be exploited to measure protein-protein interactions provided that the tryptophan undergoes an environmental change upon formation of the complex. Because neither GroEL, GroES, nor Gp31 contain tryptophan residues, we sought to introduce one such that it would report Gp31 binding to GroEL. Gp31(I36W) was created by site-directed mutagenesis. Ile^{36} is the central residue of the hydrophobic tripeptide, Leu^{35}-Ile^{36}-Ile^{37}, in the Gp31 mobile loop. Gp31(I36W) interacts with GroEL in a manner similar to wild type Gp31, consistent with the fact that it can substitute for wild type Gp31 in bacteriophage T4 growth. However, unlike

wild type Gp31, Gp31(I36W) functions with GroEL(E191G) in citrate synthase refolding (Fig. 1). Nevertheless, Gp31(I36W) can be exploited as a reporter to detect the relative binding affinities of the various GroES and Gp31 proteins in a competition assay.

The fluorescence emission spectrum of Gp31(I36W) exhibits a wavelength of maximum emission (λ_{max}) of 347 nm, which suggests that the introduced tryptophan side chain is solvent-exposed (Fig. 3*A*). The addition of GroEL in the absence of nucleotide results in a small increase in fluorescence intensity and no change in emission λ_{max}. However, further addition of ATP results in a 2-fold increase in emission intensity as well as a 10-nm decrease in λ_{max}. These results suggest that the tryptophan side chain is transferred to a nonpolar environment in the GroEL·Gp31 complex.

The relative binding affinities of Gp31 and Gp31 mutants can be evaluated with a binding competition assay. First, a complex between GroEL and Gp31 is formed in the presence of nucleotide. Subsequently, binding of Gp31(I36W) to GroEL is monitored by tryptophan fluorescence. The extent that Gp31 blocks the change in fluorescence indicates the ability of the Gp31 competitor to inhibit Gp31(I36W) binding.

Prior incubation of GroEL·ATP with Gp31 only slightly inhibits Gp31(I36W) binding (Fig. 3*B*). In contrast, Gp31(L35I) complexed with GroEL·ATP effectively blocks Gp31(I36W) binding, indicating that it is more difficult to displace than its wild type counterpart. Gp31(L35I,T31A) in complex with GroEL·ATP hinders Gp31(I36W) binding partially, neither as well as Gp31(L35I) nor as weakly as Gp31. From these experiments, the following relative order of cochaperonin binding affinity to GroEL·ATP is established: Gp31(L35I) > Gp31(L35I, T31A) > Gp31.

Because the affected residues in the GroEL mutants are distant from the mobile loop binding site, one would expect the same order of binding affinity on the GroEL mutants used in this study. We tested this prediction by repeating the same experiment while substituting GroEL with GroEL(A383T). Indeed, the order of relative affinity remains the same (data not shown).

Synthetic Mobile Loop Peptides Corresponding to Gp31 Mutants Recapitulate Altered GroEL Binding—Above we showed that mutations that affect residues in the mobile loop of Gp31 alter its affinity for GroEL. To establish that these differences are a direct result of changes in the mobile loop binding to GroEL, we compared the GroEL binding properties of synthetic peptides corresponding to the mobile loops of our Gp31 mutants by analysis of trNOEs. The appearance of trNOEs in the NOESY spectra of the three peptides in the presence of GroEL indicates that each binds to GroEL (Fig. 4). However, the Gp31(L35I) peptide exhibits more intense trNOEs compared with those of Gp31 and Gp31(L35I,T31A) peptides, suggesting that the L35I substitution strengthens mobile loop binding to GroEL and that the T31A substitution weakens it. In the presence of GroEL(E191G), there is a marked decrease in trNOEs for Gp31 and Gp31(L35I,T31A) compared with Gp31(L35I), consistent with the lack of *in vivo* interaction between GroEL(E191G) and these cochaperonins. These results indicate that the mobile loop itself can recognize the defect in GroEL(E191G) despite the relatively large distance between the altered amino acid residue and the mobile loop binding site in GroEL (Fig. 5*A*).

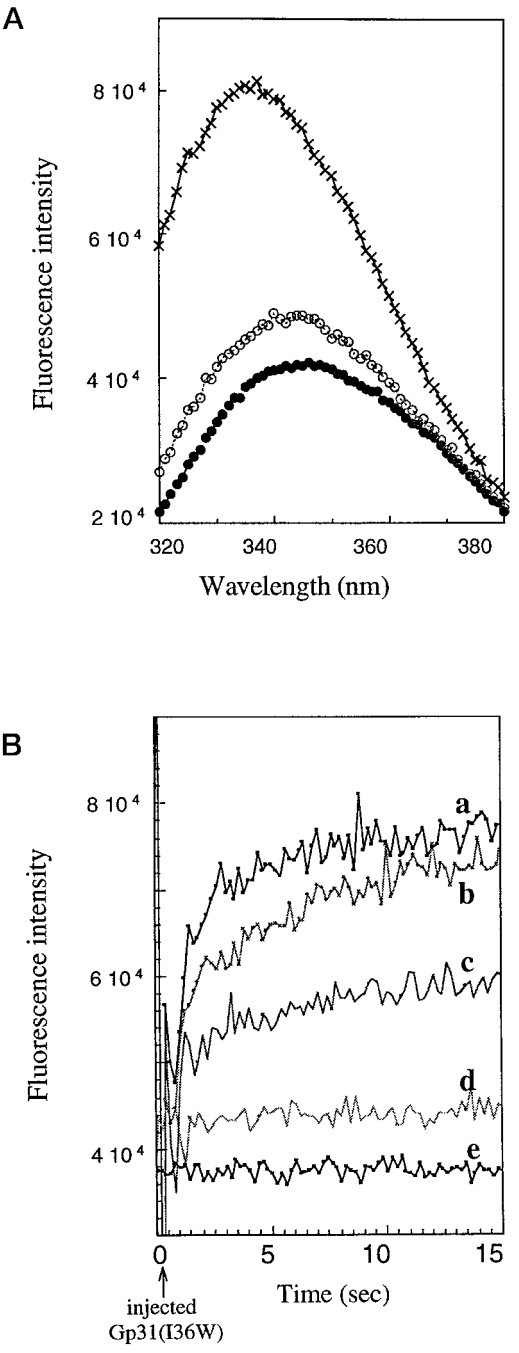

FIG. 3. **Inhibition of Gp31(I36W) binding to GroEL by Gp31 mutant proteins monitored by fluorescence.** *A*, fluorescence intensity of Gp31(I36W) is enhanced in the presence of GroEL and nucleotide. Gp31(I36W) interacts with GroEL in the presence of ATP as reported by an increase in fluorescence intensity as well as a blue shift in λmax. Tryptophan was specifically excited at 295 nm, and its emission was recorded over the range 320 to 380 nm. ●, Gp31(I36W); ○, Gp31(I36W)-GroEL; ×, Gp31(I36W)·GroEL·ATP. *B*, Gp31(I36W) was injected into a cuvette containing a preequilibrated GroEL·ATP·cochaperonin complex. *a*, GroEL + Gp31(I36W); *b*, GroEL·Gp31 + Gp31(I36W); *c*, GroEL·Gp31(L35I,T31A) + Gp31(I36W); *d*, GroEL·Gp31(L35I) + Gp31(I36W); *e*, Gp31(I36W). Tryptophan was excited at 295 nm, and time-based emission was recorded at 337 nm. In the absence of cochaperonin, Gp31(I36W) binds rapidly to GroEL·ATP. The preaddition of Gp31 does not block binding but instead retards binding of Gp31(I36W). The preaddition of Gp31(L35I) almost completely inhibits binding of Gp31(I36W), whereas the preaddition of Gp31(L35I,T31A) inhibits Gp31(I36W) binding to GroEL by ~50%.

DISCUSSION

GroEL-Gp31 Mutant-Suppressor Pairs Illustrate a Mechanism of Allele-specific Genetic Interaction—As stated earlier, taking advantage of a GroEL mutant, GroEL(A383T), that does not function with Gp31(L35I), we have isolated compensatory mutations that reveal a striking genetic interaction between Gp31 and GroEL. Specifically, all mutants of bacteriophage T4 Gp31(L35I) isolated as restoring ability to grow on

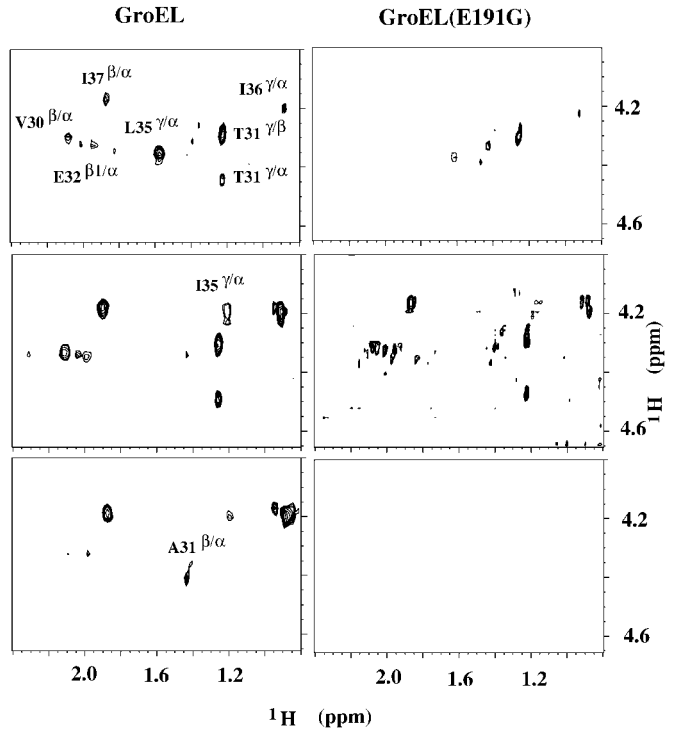

FIG. 4. **H$^\alpha$/upfield region of NOESY spectra of mobile loop peptides in the presence of GroEL.** Spectra were recorded at 30 °C as described under "Experimental Procedures."

groEL515(A383T) simultaneously lose their ability to grow on *groEL44*(E191G). Potentially, the GroEL-Gp31 genetic interaction could be ascribed to a conventional mechanism of allele specificity, in which distinct mutant-suppressor pairs arise from direct contacts among the affected amino acids in the protein-protein interface (33). However, amino acids involved in the GroEL-Gp31 genetic interactions analyzed here are located far from each other in the GroEL·Gp31 complex (Fig. 5*A*).

Our biochemical analyses of the mutant Gp31 proteins suggest that mutant-suppressor pairs complement each other by contributing in opposite ways to GroEL-Gp31 affinity. The relative affinities of wild type and mutant Gp31 proteins were probed indirectly through their ability to block binding to GroEL of a fluorescent variant of Gp31, Gp31(I36W), and by the strength of trNOEs observed for their corresponding mobile loop peptides in the presence of GroEL. Both assays indicate the following relative affinity for GroEL: Gp31(L35I) > Gp31(L35I,T31A) > Gp31. Thus, it appears that the increased GroEL binding affinity of Gp31(L35I) compensates for the low affinity interaction of the GroEL(E191G)-Gp31 pair, and the reduced affinity of Gp31(L35I,T31A) compensates for the presumed high affinity interaction of the GroEL(A383T)-Gp31(L35I) pair. The same relative affinity ranking is observed for binding of the various Gp31 proteins to GroEL(A383T) (data not shown) and for binding of the corresponding mobile loop peptides to GroEL(E191G). The fact that the order of affinity is indifferent to the GroEL protein tested supports our proposal that the mechanism of GroEL-Gp31 genetic interactions studied here arises from compensatory affinity changes rather than classical allele-specific alterations in the structure of the binding interface.

Amino Acid Substitutions in the Mobile Loop Affect Formation of the GroEL-bound Hairpin Conformation—As detailed above, the predominance of substitutions at amino acid position 31 in the pseudorevertants (14 of 20 isolates; Table I) suggests that changes at this position have a greater potential for counteracting the increased binding affinity caused by the L35I substitution. Consistent with this hypothesis, previous NMR studies detected trNOEs between the side chains of Thr^{31}

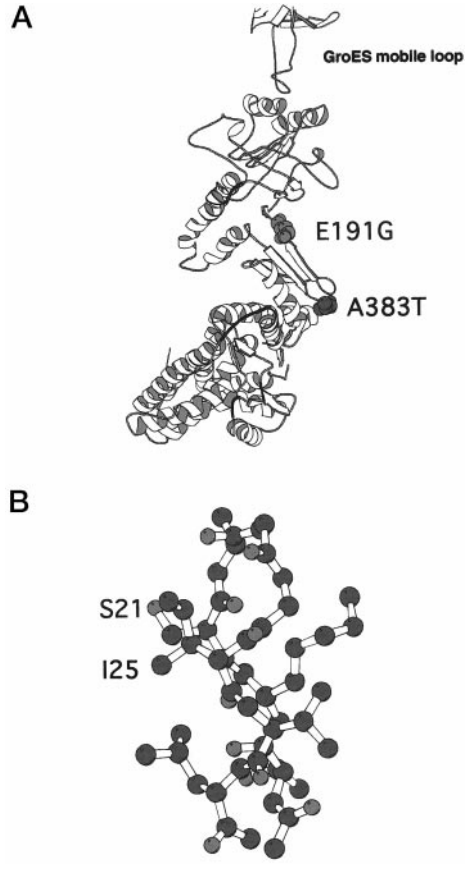

FIG. 5. **X-ray and NMR structures.** *A*, a single subunit from the GroEL·ADP·GroES crystal structure (8). The GroEL(E191G) and GroEL(A383T) specific amino acid changes are localized in the hinges flanking the intermediate domain of GroEL and are highlighted. *B*, the structure of the GroEL-bound GroES mobile loop peptide was determined by trNOE NMR in the presence of GroEL. The Ser^{21} and Ile^{25} residues (equivalent to Thr^{31} and Leu^{35} of Gp31, respectively) interact in the GroEL-bound conformation (24). Stuctures were modeled using MolScript (44).

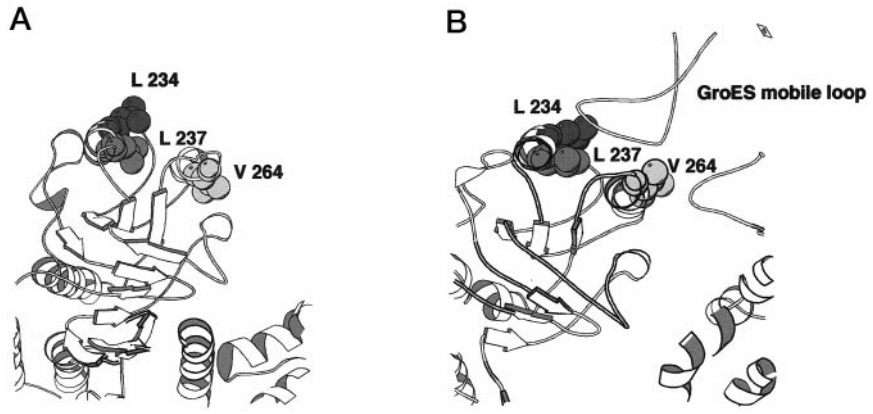

FIG. 6. **Location of GroEL residues directly bound by the GroES mobile loop.** Residues Leu[234], Leu[237], and Val[264] are presented as *space-filled* atoms. *A*, a close-up view of the apical domain in the GroEL crystal structure (3). *B*, a close-up view of the GroEL apical domain with the GroES mobile loop in the GroEL·ADP·GroES crystal structure (8). Structures were modeled using MolScript (44).

and Leu[35] in the Gp31 mobile loop peptide bound to GroEL, indicating that these side chains approach within a few angstroms of each other (24). The proposed Thr[31]-Leu[35] contact corresponds to the Ser[21]-Ile[25] contact observed in the GroEL-bound GroES mobile loop peptide (23). All of the trNOE data in the Gp31 peptide were consistent with its forming the same 3:5 hairpin conformation (using the classification of Sibanda and Thornton (34)) as that formed by the corresponding GroES mobile loop peptide (Fig. 5*B*), which places these two side chains next to each other but on opposite strands of the hairpin.

Amino acid β-strand preferences can account for the observed changes in GroEL-Gp31 binding caused by the various mutations. A host-guest study ranked all 20 amino acids by the change in free energy for folding of a protein in which the substituted site was located at the edge of a β-sheet (35). This study may be the most relevant because a β-hairpin more closely resembles the edge than the middle of a β-sheet. It was found that Leu is unfavorable for β-sheet formation, Ala and Ile are neutral, whereas Thr is favorable. Thus, the L35I substitution is expected to increase β-hairpin stability, whereas either T31A or T31I are expected to decrease β-hairpin stability. Because Gp31 binding to GroEL is coupled to β-hairpin formation, changes in GroEL binding affinity may result from changes in β-hairpin stability. Minor and Kim (35) noted a significant difference in the rank order of amino acids in β-sheet propensity for substitution at the edge of a β-sheet *versus* the middle of a β-sheet. In particular, Ile is a strong β-sheet-former in the middle of a β-sheet but essentially neutral at its edge. The authors suggested this is because of a balance of a favorable contribution from side chain conformational entropy and poor hydrophobic burial at the edge of the β-sheet. Thus, the initially surprising result that either the T31A or T31I substitution can result in the same phenotype can now be understood in terms of contributions to β-sheet stability.

Our experimental results, coupled with the conclusions derived from the model systems discussed above, demonstrate that the GroEL-Gp31 genetic interaction can be understood in the framework of a folding transition by the Gp31 mobile loop. The mobile loop conformational dynamics must be exquisitely poised for folding into a β-hairpin and yet sufficiently disordered that GroEL binding is not too tight. As a result, seemingly subtle amino acid substitutions, such as L35I, can completely rescue or block bacteriophage T4 growth depending on the particular mutant host.

Amino Acid Substitutions in the GroEL Hinge Regions Affect Local as Well as Large Scale Conformational Changes—Substitutions in the hinges could change the distribution of GroEL subunits between apical domain-open and apical domain-closed conformations and/or affect the apical domain-mobile loop docking interaction by allosteric communication. We compared the relative orientation of the three GroEL apical domain residues that contact the mobile loop in the crystal structure of GroEL·ADP·GroES with the orientation of these residues in the crystal structure of GroEL alone (Fig. 6 (8, 36)). The orientation of the Val[264] side chain is shifted with respect to other apical domain residues, suggesting that the α-helix containing Val[264] twists when GroEL visits its open conformation. The other two GroEL residues, Leu[234] and Leu[237], show minor changes in orientation. Because mobile loop peptides exhibit reduced binding to GroEL(E191G), mobile loop and, therefore, Gp31 binding may be controlled by the ratio of open *versus* closed GroEL subunits. If the mobile loop has a lower affinity for GroEL in the closed conformation and GroEL(E191G) visits the open state less frequently, then poor binding of Gp31 could be because of a smaller population of GroEL(E191G) subunits in the open state.

Implications for Protein-Protein Interaction—An affinity-based mechanism for allele specificity has been ascribed to other protein-protein interactions, raising the possibility that the classical notion of allele-specificity is generally avoided by robust, flexible protein-protein contacts. For example, suppression of defects in fimbrin-actin interactions in yeast has been attributed to a global increase in affinity of fimbrin mutants for actin mutants, and at least two fimbrin mutants bind more tightly to wild type actin (37). Crystal structures of human fimbrin and bovine actin reveal that residues affected in the mutant yeast proteins are not only localized to surfaces of potential protein-protein contact, and several are buried in a hydrophobic core (38). In the bacterial chemotaxis system, interaction of the response regulator CheY with the receptor kinase CheA has been localized to a surface of CheY, but residues in the contact surface are not evolutionarily conserved, and crystal structures of CheY with the P2 domain of CheA reveal at least three different modes of binding (39, 40). In the chaperonin system, we find that mutations affecting GroEL-Gp31 affinity modulate a folding transition in the Gp31 mobile loop. Hence, in all of these systems, residues in the intermolecular interfaces may be less critical than residues controlling domain folding and stability.

Strict allele-specificity may always involve a conformational switch in one partner of a protein-protein interacting pair. In the chemotaxis system, bias for clockwise *versus* counter-clockwise motor rotation is controlled by interactions of phospho-CheY with the flagellar switch protein FliM. Many, if not all mutations in FliM that suppress mutations in CheY are thought to adjust the bias of the switch rather than restore normal interactions with mutant CheY (41, 42). The indirect effect of these suppressor mutations in FliM is analogous to the effect of hinge mutations in GroEL that compensate for strong or weak binding by mobile loop mutants in Gp31. Apparently, a great deal of redundancy has accumulated in the structural

features of protein-protein interactions, as has already been appreciated in protein folding itself (43). Mutations tend to shift conformational equilibria between broad energy minima rather than cause distinct changes in structure.

Acknowledgments—We thank Dr. Gisou van der Goot for her hospitality and help in using the luminescence spectrometer, Dr. Karol Maskos for help with NMR experiments, Dr. Alistair Kippen for help with the electrospray mass spectroscopy determinations, Françoise Schwager for assistance in DNA sequencing, Drs. Matthias Mayer, Jill Zeilstra-Ryalls, and Olivier Fayet for providing plasmids, Dr. Maciej Zylicz with help in protein overexpression, and Dr. David Boisvert for critical reading of the manuscript.

REFERENCES

1. Hartl, F. U. (1996) *Nature* **381,** 571–580
2. Ewalt, K. L., Hendrick, J. P., Houry, W. A., and Hartl, F. U. (1997) *Cell* **90,** 491–500
3. Braig, K., Otwinowski, Z., Hegde, R., Boisvert, D. C., Joachimiak, A., Horwich, A. L., and Sigler, P. B. (1994) *Nature* **371,** 578–586
4. Hendrix, R. W. (1979) *J. Mol. Biol.* **129,** 375–392
5. Hohn, T., Hohn, B., Engel, A., and Wurtz, M. (1979) *J. Mol. Biol.* **129,** 359–373
6. Hunt, J. F., Weaver, A. J., Landry, S. J., Gierasch, L., and Diesenhofer, J. (1996) *Nature* **379,** 37–45
7. Tilly, K., Murialdo, H., and Georgopoulos, C. (1981) *Proc. Natl. Acad. Sci. U. S. A.* **78,** 1629–1633
8. Xu, Z., Horwich, A. L., and Sigler, P. B. (1997) *Nature* **388,** 741–750
9. Roseman, A. M., Chen, S., White, H., Braig, K., and Saibil, H. R. (1996) *Cell* **87,** 241–251
10. Todd, M. J., Viitanen, P. V., and Lorimer, G. H. (1994) *Science* **265,** 659–666
11. Rye, H. S., Burston, S. G., Fenton, W. A., Beechem, J. M., Xu, Z., Sigler, P. B., and Horwich, A. L. (1997) *Nature* **388,** 792–798
12. Hayer-Hartl, M. K., Weber, F., and Hartl, F. U. (1996) *EMBO J.* **15,** 6111–6121
13. Weissman, J. S., Hohl, C. M., Kovalenko, O., Kashi, Y., Chen, S., Braig, K., Saibil, H., Fenton, W. A., and Horwich, A. L. (1995) *Cell* **83,** 577–587
14. Bukau, B., and Horwich, A. L. (1998) *Cell* **92,** 351–366
15. Fenton, W. A., and Horwich, A. L. (1997) *Protein Sci.* **6,** 743–760
16. Richardson, A., Landry, S. J., and Georgopoulos, C. (1998) *Trends Biochem. Sci.* **23,** 138–143
17. Georgopoulos, C., Hendrix, R. W., Kaiser, A. D., and Wood, W. B. (1972) *Nat. New Biol.* **239,** 38–41
18. Laemmli, U. K., Beguin, F., and Gujer-Kellenberger, G. (1970) *J. Mol. Biol.* **47,** 69–85
19. Georgopoulos, C. (1992) *Trends Biochem. Sci.* **17,** 295–299
20. van der Vies, S. M., Gatenby, A. A., and Georgopoulos, C. (1994) *Nature* **368,** 654–656
21. Koonin, E. V., and van der Vies, S. (1995) *Trends Biochem. Sci.* **20,** 14–15
22. Hunt, J. F., van der Vies, S. M., Henry, L., and Deisenhofer, J. (1997) *Cell* **90,** 361–371
23. Landry, S. J., Zeilstra-Ryalls, J., Fayet, O., Georgopoulos, C., and Gierasch, L. M. (1993) *Nature* **364,** 255–258
24. Landry, S. J., Taher, A., Georgopoulos, C., and van der Vies, S. (1996) *Proc. Natl. Acad. Sci. U. S. A.* **93,** 11622–11627
25. Zeilstra-Ryalls, J., Fayet, O., and Georgopoulos, C. (1994) *J. Bacteriol.* **176,** 6558–6565
26. Keppel, F., Lipinska, B., Ang, D., and Georgopoulos, C. (1990) *Gene* **90,** 19–25
27. Zeilstra-Ryalls, J., Fayet, O., Baird, L., and Georgopoulos, C. (1993) *J. Bacteriol.* **175,** 1134–1143
28. Repoila, F., Tétart, F., Bouet, J.-Y., and Krisch, H. M. (1994) *EMBO J.* **13,** 4181–4192
29. Mayer, M. P. (1995) *Gene* **163,** 41–46
30. Kunkel, T. A., Bebenek, K., and McClary, J. (1991) *Methods Enzymol.* **204,** 125–139
31. Guzman, L.-M., Belin, D., Carson, M. J., and Beckwith, J. (1995) *J. Bacteriol.* **177,** 4121–4130
32. Zhi, W., Landry, S. J., Gierasch, L. M., and Srere, P. A. (1992) *Protein Sci.* **1,** 522–529
33. Parkinson, J. S., and Parker, S. R. (1979) *Proc. Natl. Acad. Sci. U. S. A.* **76,** 2390–2394
34. Sibanda, B. L., and Thornton, J. M. (1991) *Methods Enzymol.* **202,** 59–82
35. Minor, D. L., Jr., and Kim, P. S. (1994) *Nature* **371,** 264–267
36. Braig, K., Adams, P. D., and Brünger, A. T. (1995) *Nat. Struct. Biol.* **2,** 1083–1094
37. Sandrock, T. M., O'Dell, J. L., and Adams, A. E. (1997) *Genetics* **147,** 1635–1642
38. Goldsmith, S. C., Pokala, N., Shen, W., Fedorov, A. A., Matsudaira, P., and Almo, S. C. (1997) *Nat. Struct. Biol.* **4,** 708–712
39. McEvoy, M. M., Hausrath, A. C., Randolph, G. B., Remington, S. J., and Dahlquist, F. W. (1998) *Proc. Natl. Acad. Sci. U. S. A.* **95,** 7333–7338
40. Welch, M., Chinardet, N., Mourey, L., Birck, C., and Samama, J. P. (1998) *Nat. Struct. Biol.* **5,** 25–29
41. Roman, S. J., Meyers, M., Volz, K., and Matsumura, P. (1992) *J. Bacteriol.* **174,** 6247–6255
42. Sockett, H., Yamaguchi, S., Kihara, M., Irikura, V. M., and Macnab, R. M. (1992) *J. Bacteriol.* **174,** 793–806
43. Bowie, J. U., Reidhaar-Olson, J. F., Lim, W. A., and Sauer, R. T. (1990) *Science* **247,** 1306–1310
44. Kraulis, P. J. (1991) *J. Appl. Crystallogr.* **24,** 946–950